Global Distribution of Maximum Land Surface Temperature Inferred from Satellites.

Dr Fred Prata
CSIRO Atmospheric Research
Aspendale, Victoria, Australia

26 May, 2000

1 Background

Land surface temperatures derived from satellites rely on infrared measurements made within the 10–12 μm window. The radiometers that make these measurements use data collection methods that limit both the resolution and dynamic range of the digital data. The digitisation of the data affects the lowest and highest radiances that can be recorded. The lowest values are generally not cause for concern because the calibration system allows the radiometer to view cold space at around 4 K, and therefore radiances can be measured for the minimum temperatures encountered on earth. There are restrictions on the highest temperatures recorded.

The effects on the highest temperatures recorded are partially offset by acquiring data at times when the size of solar heating of the land surface is not extreme and by absorption of radiation by water vapour which reduces the radiances received at the satellite radiometer.

This note examines the global distribution of land surface temperatures to derive regions and times (on a monthly basis) when a satellite-borne radiometer will encounter extreme high surface temperatures. The source of data is the "World Land Surface Temperature Atlas" (ESA, 1998), derived from AVHRR radiances during the year 1992-1993. Only the climatic data set is considered at monthly time-scale and 0.5° x 0.5° latitude-longitude resolution. The discussion is limited to saturation problems in the split-window channels. Saturation can also occur at 3.7 μm through a combination of hot land surfaces and high solar reflection–a likely scenario over bright desert surfaces.

2 The problem

The Advanced Along Track Scanning Radiometer (AATSR) on board the ENVISAT satellite will make global thermal infrared measurements of the earth's surface. The nominal daytime overpass time will be 10:30 LT (local time). Even though this is well before the time of maximum heating of the surface, it has been noticed that over semi-arid and arid land surfaces during the summer, land surface temperatures can exceed 65 °C, or roughly 20 °C higher than the saturation temperature of the ATSR-2 thermal infrared channels. The theoretical maximum land surface temperature possible has been estimated by Garratt (1992) to be around 80-90 °C.

Saturation has been observed in the AVHRR split-window channels and saturation temperatures for the AVHRR instruments are shown in Table 1.

Table 1: **Saturation temperatures (°C) for channels 4 and 5 of the AVHRRs on-board the NOAA-7, NOAA-9, NOAA-11 and NOAA-12 satellites. The saturation temperature corresponds to a count reading of 0, and varies because the calibration slopes and intercepts vary.**

Satellite	Channel 4 (11 μm) Saturation temperature	Channel 5 (12 μm) Saturation temperature
NOAA- 7	50	53
NOAA- 9	50	57
NOAA-11	60	55
NOAA-12	51	53

3 Satellite Data

Figure 1 shows an ATSR-2 thermal infrared image of central Australia which illustrates the saturation problem. There are large areas of the image where the 11 μm temperature has reached its maximum recordable value ($\approx$319 K).

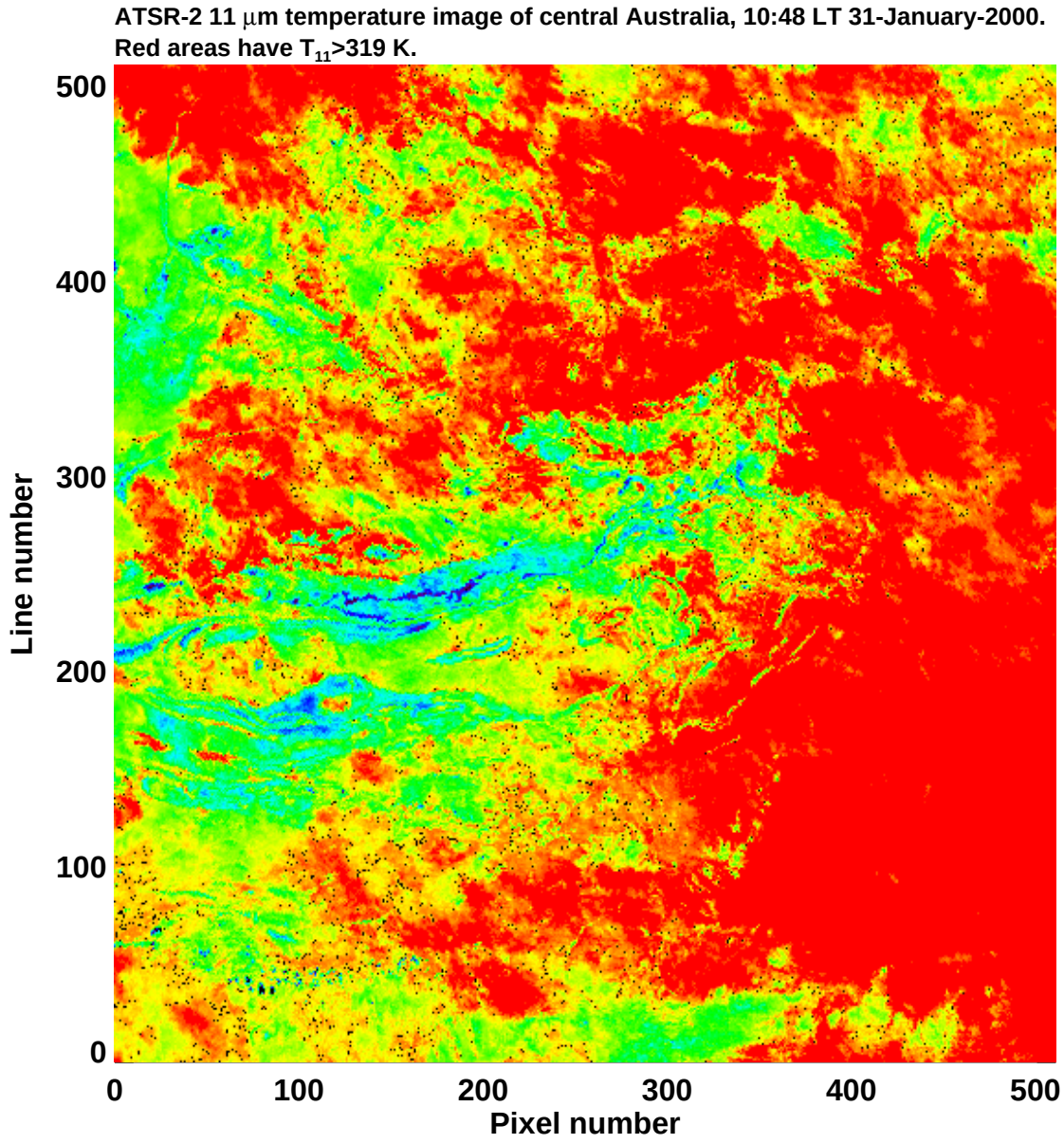

Figure 1. ATSR-2 11 μm brightness temperature image of central Australia. The range of temperatures represented is 305–319 K. Areas where the saturation limit has been reached ($\approx$319 K) are shown in red.

The frequency distribution for this image is shown in Figure 2. About 35% of the pixels in this image are saturated.

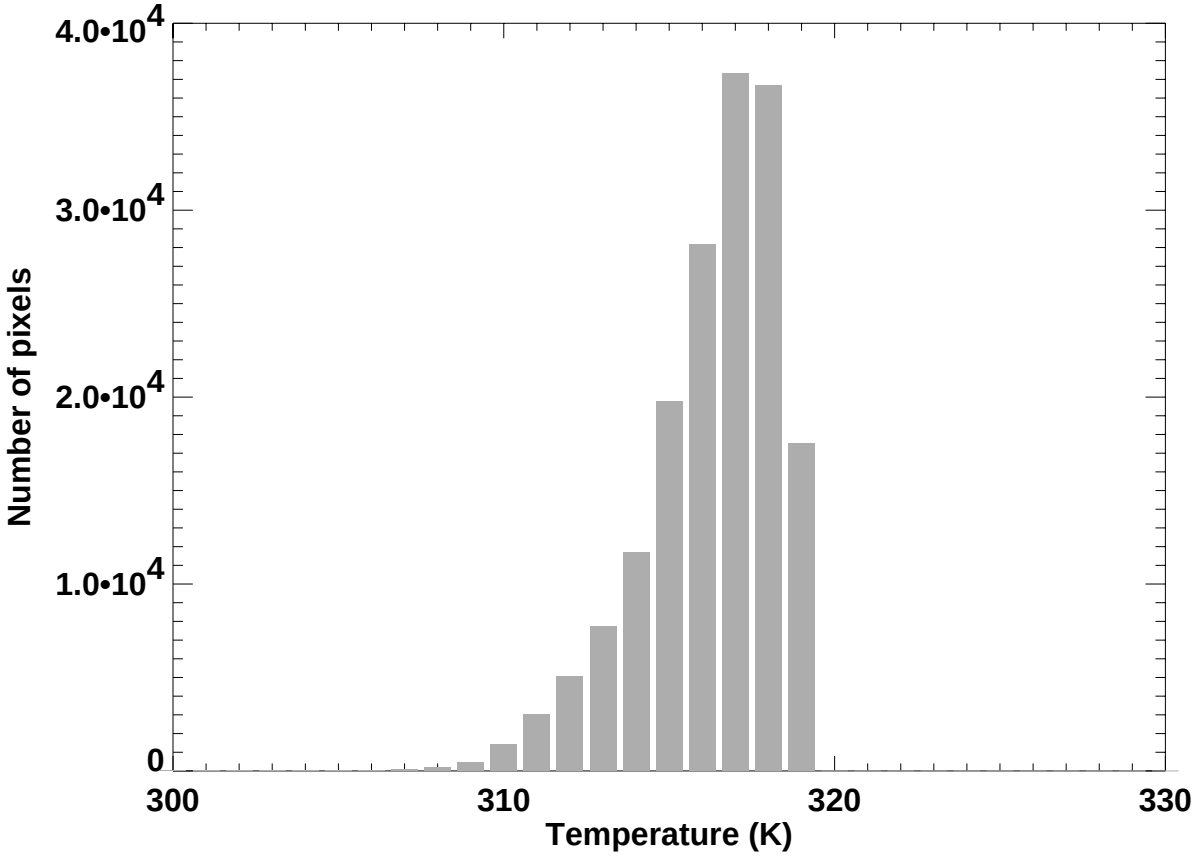

Figure 2. Frequency distribution of temperatures for the ATSR-2 image shown in Figure 1.

To investigate the frequency and spatial distribution of this problem, satellite estimates of land surface temperatures from the AVHRR are used to derive monthly global maps showing the regions where saturation is most likely to occur. The source of data for this study is the "World Land Surface Temperature Atlas" (ESA, 1998) on CD-ROM (which we shall refer to as the WLSTA) which contains 12 months of so-called climatic land surface temperatures. These are monthly composites of surface temperatures from the AVHRR instruments during the year 1992-1993. The compositing operates on 1 km scale data and 10-day time intervals and only daytime orbits are used. The data are aggregated to 0.5° x 0.5° latitude-longitude resolution (about 50 km x 50 km at the equator). The compositing algorithm and cloud screening methods are given in the accompanying documents describing the data-set.

4 Land Surface Temperature Algorithm

After an extensive survey of existing algorithms the authors of the WLSTA chose to use an algorithm due to Ulivieri *et al.* (1994). This is a split-window algorithm with the following form,

$$LST = T_{11} + 2.76(T_{11} - T_{12}) + 38.6(1 - \epsilon) - 96\Delta\epsilon, \quad (1)$$

where T_{11} and T_{12} are the channel 4 and channel 5 AVHRR brightness temperatures, ϵ is the mean emissivity of the surface at 11 and 12 μm and $\Delta\epsilon$ is the emissivity difference at these wavelengths. The emissivity and its variability are not known for the global earth's surface. The authors used a surrogate, the NDVI, to estimate emissivity. The purpose of this note is not to examine the effectiveness of their approach, and we will assume that this algorithm is representative of the class of split-window algorithms currently in use to estimate land surface temperatures. The validation of the algorithm was difficult because of the lack of good ground-truth data for the 1992-1993 period. Nevertheless the authors have done the best analysis possible given the constraints. It is difficult to ascertain the accuracy of the retrievals, but from experience it is known that daytime estimates of LST from the AVHRR are at best accurate to 2-3 K (Prata, 1994). Using monthly means would reduce the rms errors of the retrievals but biases may still be large. A conservative estimate of the bias accuracy of the retrieval is $\pm$ 3 K.

5 Sampling Considerations

Figure 3(a) shows a plot of the diurnal variation of land surface temperature measured at a semi-arid site in Australia (Amburla, 23.4° S, 133.1 ° E) in the height of summer. The vertical lines on this plot represent the nominal overpass times of the AVHRR and ATSR-2/AATSR instruments at the site. Shaded regions show parts of the temperature cycle where the instruments saturate (red for the AVHRR and yellow for the ATSR-2/AATSR). Both instruments would be saturated on this day. For the ATSR-2/AATSR, the temperature difference between the observed temperature and the point of saturation is about 7 °C and about 4 °C for the AVHRR.

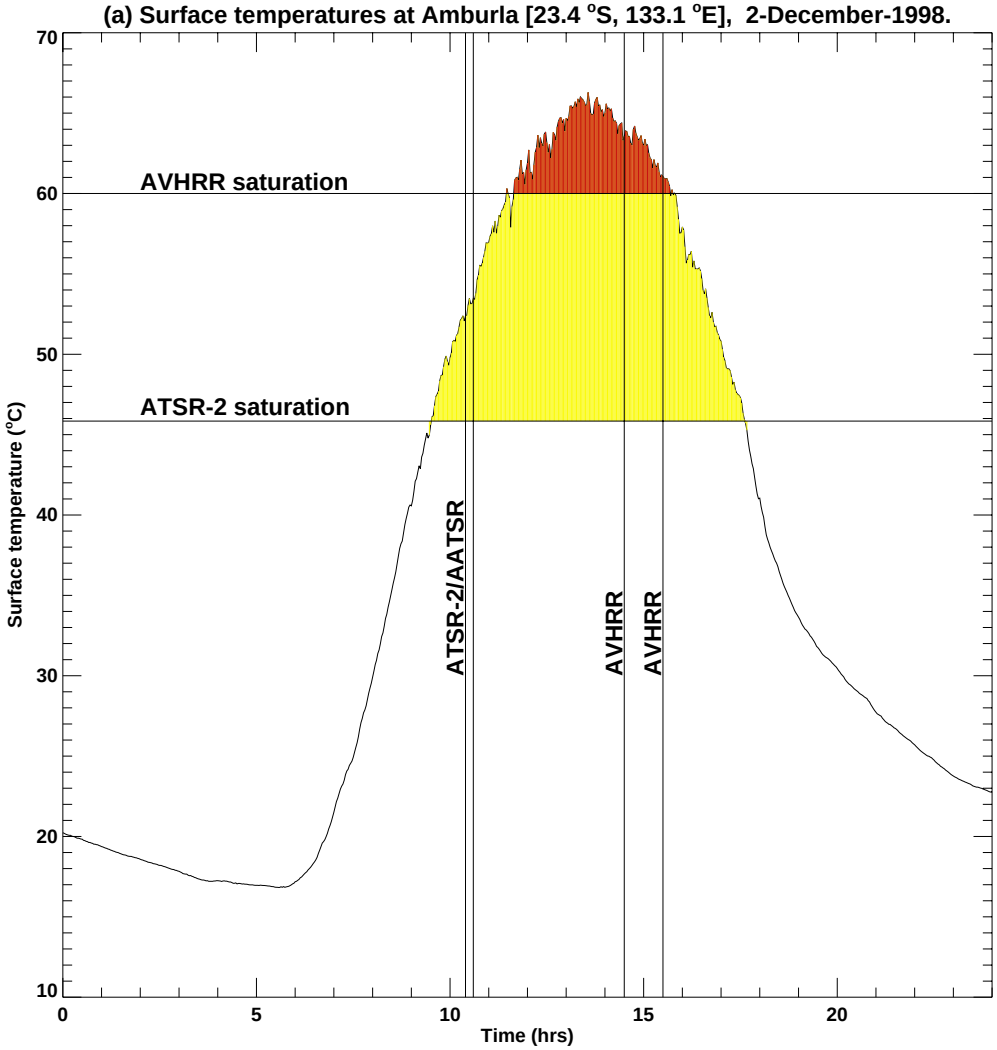

Figure 3 (a). The diurnal land surface temperature cycle at Amburla, NT, Australia during a clear day in summer. The vertical lines show the nominal overpass times of the ATSR-2/AATSR and the AVHRR. The horizontal lines show the current saturation temperatures of the 11 μm channels.

Saturation is more likely for the ATSR-2/AATSR than the AVHRR because the saturation temperature is lower. However, the later sampling time of the AVHRR means that it will generally record higher temperatures. Figure 3(b) shows the diurnal temperature cycle measured by an infrared radiometer mounted above a grassland site in Australia (Uardry, 34.4 ° S, 145.3 ° E), also in summer. On this occasion the AVHRR is not saturated, while the ATSR-2/AATSR is at the point of saturation. This is a typical summer's day and it is likely that on extreme days saturation would be reached for both instruments, even at this grassland site.

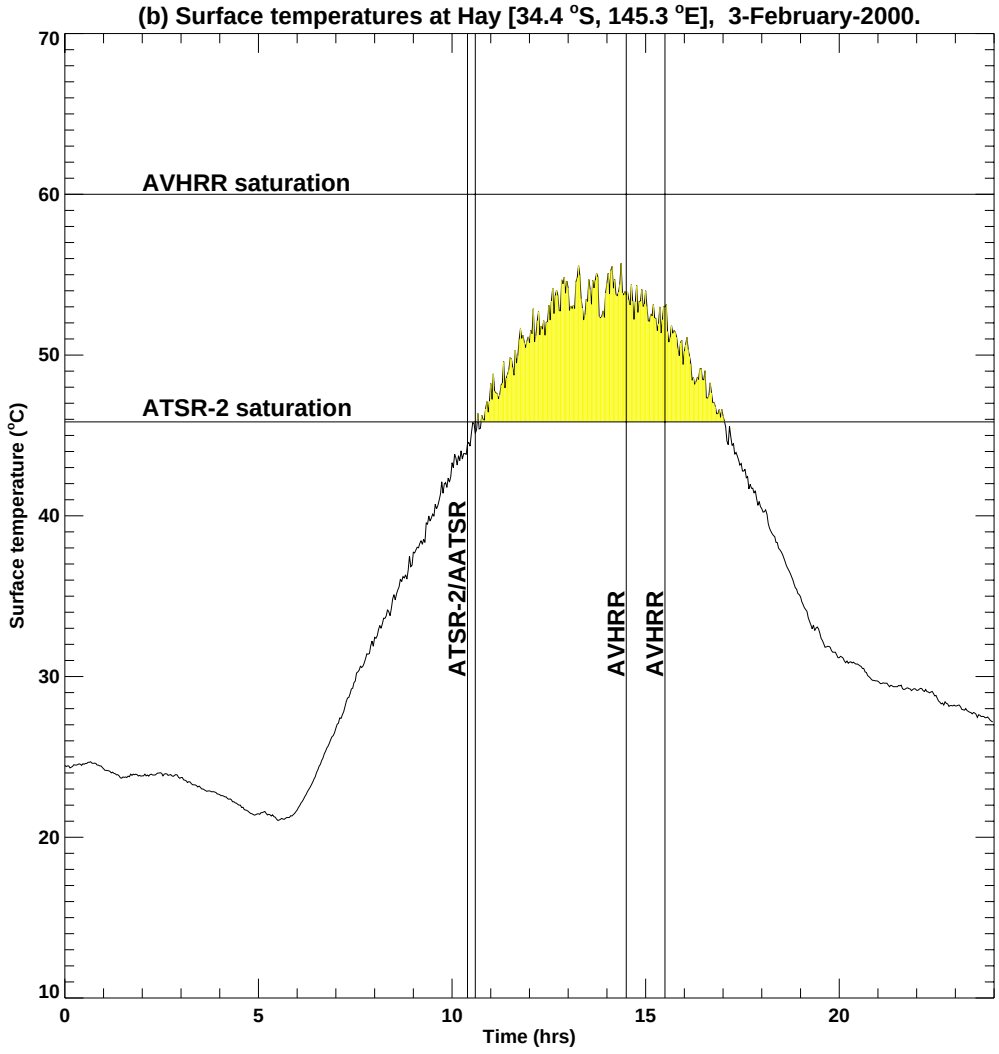

Figure 3 (b). The diurnal land surface temperature cycle at Uardry, NSW, Australia during a clear day in summer. The vertical lines show the nominal overpass times of the ATSR-2/AATSR and the AVHRR. The horizontal lines show the current saturation temperatures of the 11 μm channels.

Since we are concerned with the maximum likely temperature at 10:30 LT and we are using data obtained between 14:30 and 15:30 LT, we must account for this sampling time difference when estimating the spatial patterns of maximum temperature. The mean difference between the temperature at 14:30 LT and 10:30 LT for clear days at Amburla and Uardry is about $+6$ °C. This varies by -1 °C to $+4$ °C, depending on the individual day. Amburla is in a semi-arid environment and is typical of the hottest regions of continental Australia. Uardry is a grassland site and encounters occasional extremes of temperature. These sites can be taken as reasonable samples for global conditions. The semi-arid/arid regions are most likely to reach high temperatures and inland sites might experience extremes of temperature.

6 Saturation Maps

The spatial distribution of regions that are likely to saturate the AATSR thermal channels has been determined for mean monthly conditions. The saturation limit is determined from:
(1) The current saturation temperature for the ATSR-2 (at 10:30 LT) is $\approx$319 K.
(2) The satellite data are biassed by $\pm$3 K, the lower value being the relevant value in this case.
(3) The temperature difference at 14:30 LT and 10:30 LT is $\approx$ 5-10 K.
(4) The effect of atmospheric absorption will depress the 'sensed' brightness temperature at the satellite by 2-4 K; the lower value is used.
(5) The emissivity of the surface will reduce the magnitude of the radiance 'sensed' at the satellite. This may be from 2–5 K for sparsely vegetated or sandy surfaces (e.g. deserts). Again, we use the lower value.

Thus, the WLSTA temperature equivalent to that which would saturate the AATSR 11 μm channel (the 12 μm temperature would be similar, but usually less for those surfaces where saturation will occur) is,

$$T_{sat} = 319 - 3 + 5 + 2 + 2 = 325K.$$

The maps are shown in Figures 4–9; two months to each Figure. Regions of the land coloured grey in these maps represent areas of missing data, either because of problems with instrument coverage or persistent cloud contamination. It is apparent form the distribution of the areas identified as saturated that the problem of missing land data is inconsequential to the aim of this study.

7 Discussion and Recommendations

Saturation of the AATSR 11 and 12 μm channels is likely to occur somewhere over the land surface all of the time. The spatial distribution of regions over the globe where it is most likely to occur has been determined using AVHRR data during 1992-1993. Monthly composited products have been used and these are likely to represent a conservative lower limit on this distribution. Using an upper limit of 'actual' land surface temperature of 325 K for saturation, the total land area affected by month is summarised in Table 2. These results and

Table 2: **Total land area that reaches land surface temperatures greater than or equal to 325 K. The percentage of the total land area affected is shown in brackets.**

Month	Area (10^6 km^2)	Month	Area (10^6 km^2)
July 1992	3.395 (1.74 %)	January 1993	1.883 (0.96 %)
August 1992	3.335 (1.71 %)	February 1993	0.753 (0.39 %)
September 1992	0.475 (0.24 %)	March 1993	0.473 (0.24 %)
October 1992	0.108 (0.06 %)	April 1993	0.263 (0.13 %)
November 1992	0.540 (0.28 %)	May 1993	1.200 (0.61 %)
December 1992	2.097 (1.07 %)	June 1993	2.808 (1.44 %)

the maps shown in Figs. 4–9 suggest that a maximum of less than 2 % of the land surface is affected by saturation, but the areas affected are consistently the same regions in each hemisphere. These areas include all of the major deserts, some parts of the Russian steppes, the Indian subcontinent and large areas of semi-arid lands, typified by Saudi Arabia and inland Australia in the summer months. Consequently, although the total land area affected is small, if saturation is allowed to occur measurements over some parts of the earth in summer will always be unusable.

The data analysed in this study cannot be used to suggest the likely maximum surface temperatures encountered on earth because of saturation effects in the AVHRR. Measurements of 65 °C (≈338 K) are often reached in the Australian outback and theoretical values may exceed this by 10–15 °C, although only under extreme conditions. A practical saturation limit might be set at 330 K, which would then permit measurements in all of the hottest regions, most of the time. Assuming that the AATSR high gain mode can be used without compromising other operations, a possible strategy would be to use it between certain latitude bands at certain times of the year. Table 3 provides one possible strategy.

Table 3: **Suggested latitude bands for using the AATSR high gain mode by month.**

Month	Latitude zone	Month	Latitude zone
July	15 °N–45 °N	January	40 °S–10 °S
August	15 °N–45 °N	February	40 °S–15 °S; 0 °–15 °N
September	15 °N–45 °N; 20 °S–10 °S	March	30 °S–15 °S; 0 °–30 °N
October	10 °N–20 °N; 30 °S–10 °S	April	30 °S–15 °S; 0 °–30 °N
November	30 °S–10 °S	May	10 °N–30 °N
December	40 °S–10 °S	June	10 °N–45 °N

Refinements to this strategy could be made by also limiting the high gain acquisitions to longitude zones. Ideally, the intersections of the AATSR swaths with the land regions identified in this note could be used to trigger the high gain mode. This could be done using a reflectance threshold on one of the visible channels

since only daytime data are affected by this problem. The affects of using the high gain mode on collection of other measurements (e.g. cloud measurements over hot land surfaces) have not been considered here.

8 References

ESA, 1998, World Land Surface Temperature Atlas 1992-1993 CD-ROM, *European Space Agency*, (Contacts: Olivier.Arinoesrin.esa.it and Yann.Kerrcesbio.cnes.fr).

Garratt, J. R., 1992, Extreme maximum land surface temperatures, *J. Appl. Meteorol.*, **31**, 1096–1105.

Prata, A.J., 1994, Land surface temperatures dervied from the AVHRR and ATSR, 2, Experimental and validation of AVHRR algorithms, *J. Geophys. Res.*, **99**, 13,025–13,058.

Ulivieri, C., Castronuovo, M. M., Francioni, R., and Cardillo, C., 1994, A plit-window algorithm for estimating land surface temperature from satellites, *Adv. Space Res.*, **14**(3), 59–65.

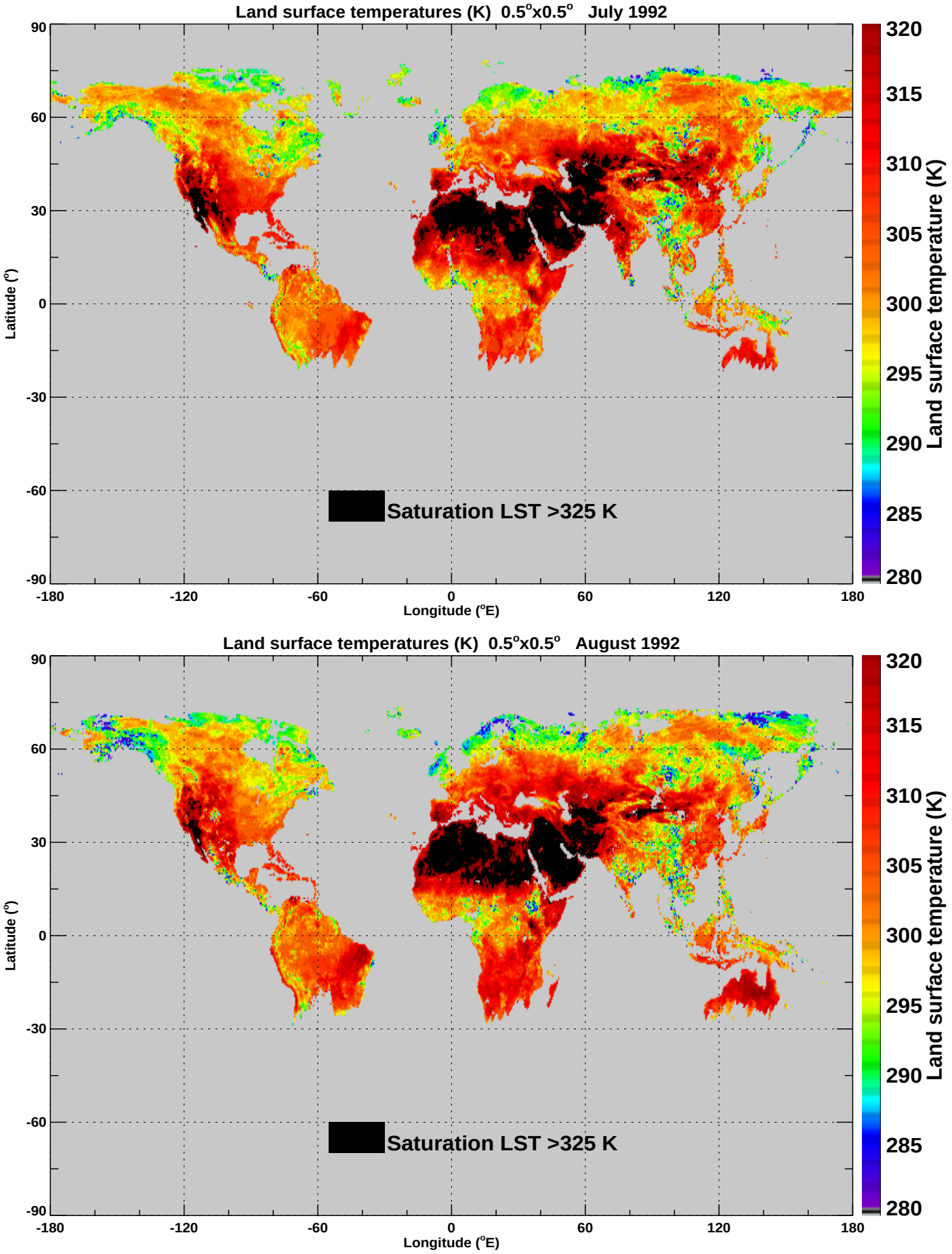

Figure 4. Global land surface temperatures inferred from satellite. Regions where the AATSR 11 μm channel is likely to saturate are coloured black. July and August 1992.

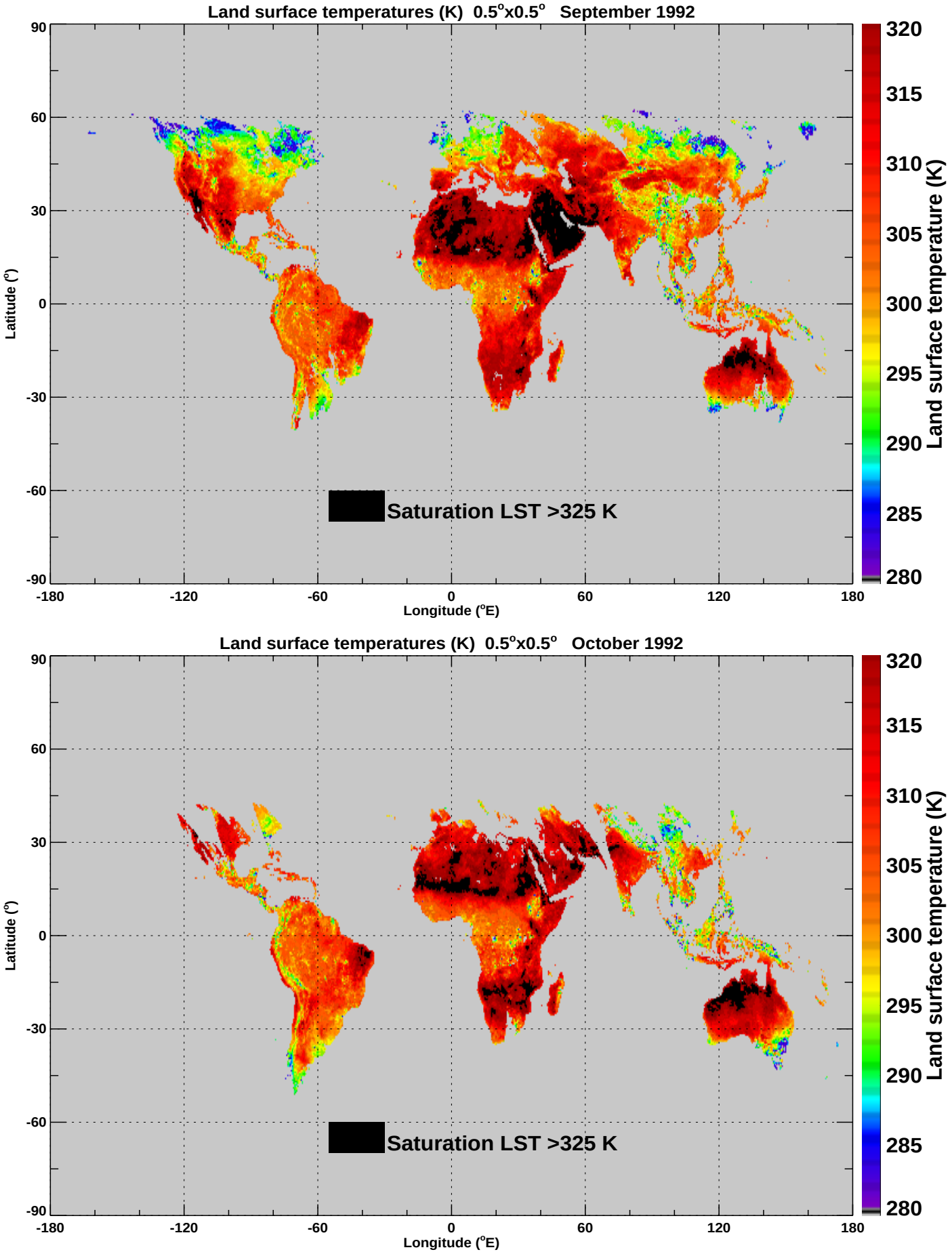

Figure 5. Global land surface temperatures inferred from satellite. Regions where the AATSR 11 μm channel is likely to saturate are coloured black. September and October 1992.

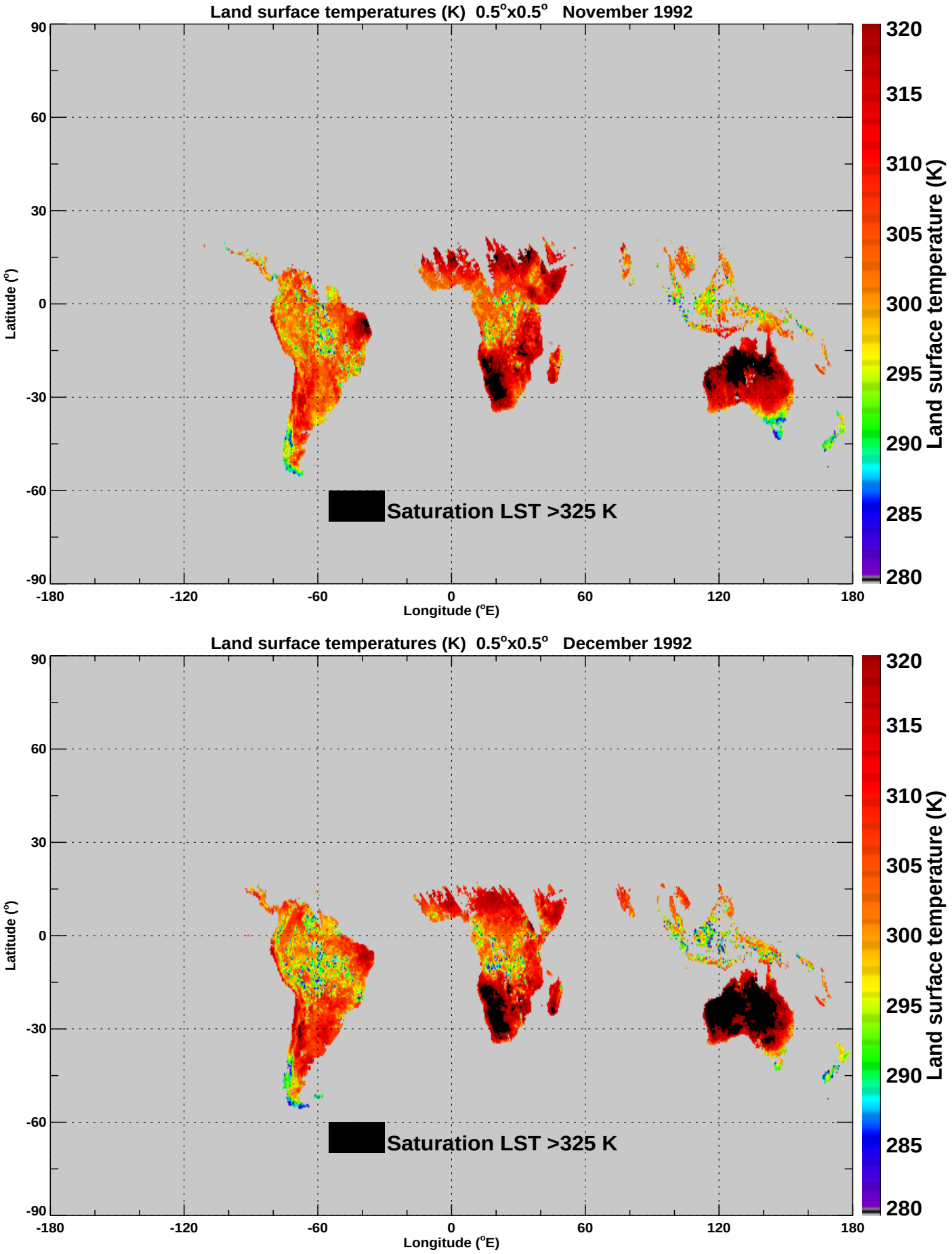

Figure 6. Global land surface temperatures inferred from satellite. Regions where the AATSR 11 μm channel is likely to saturate are coloured black. November and December 1992.

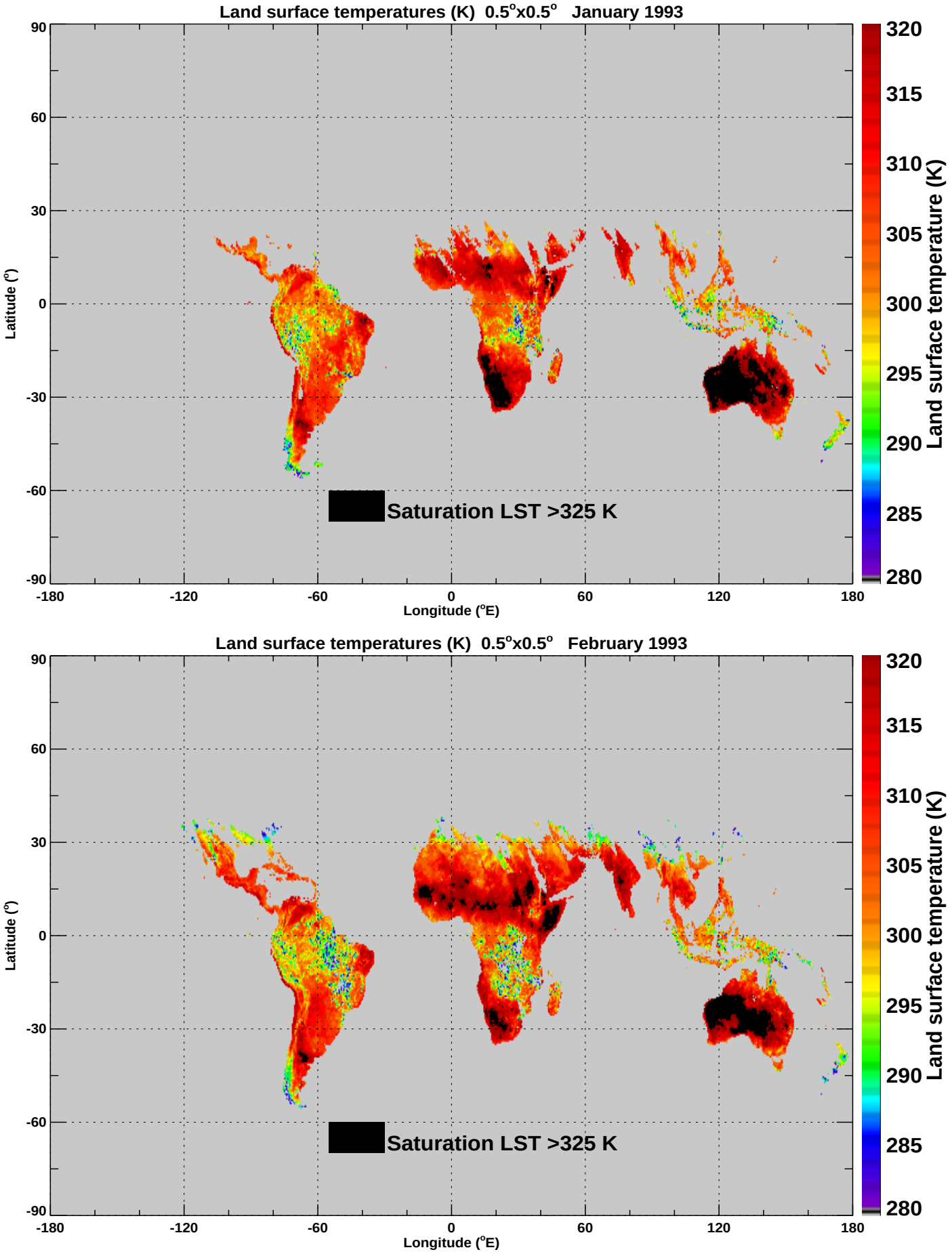

Figure 7. Global land surface temperatures inferred from satellite. Regions where the AATSR 11 μm channel is likely to saturate are coloured black. January and February 1993.

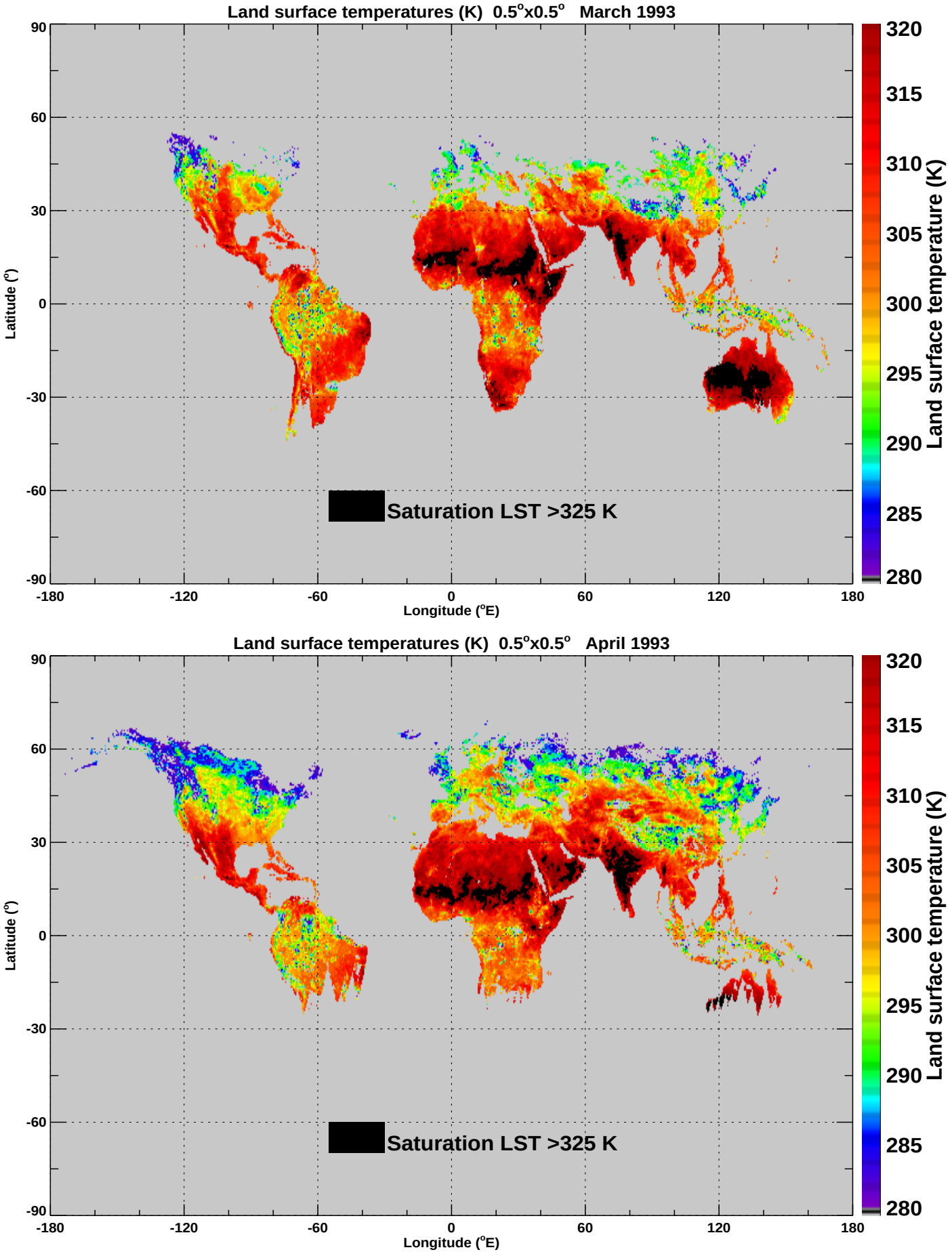

Figure 8. Global land surface temperatures inferred from satellite. Regions where the AATSR 11 μm channel is likely to saturate are coloured black. March and April 1993.

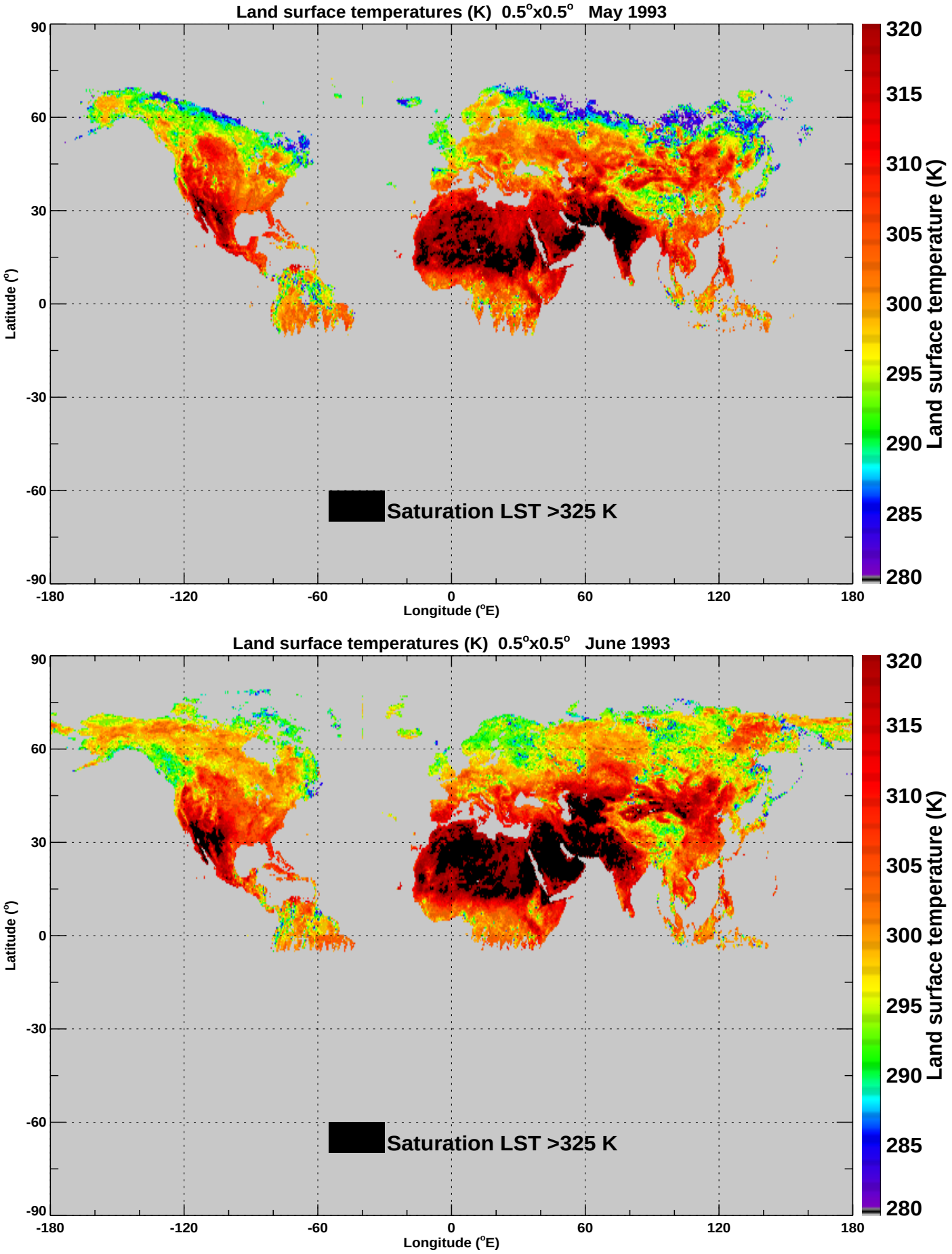

Figure 9. Global land surface temperatures inferred from satellite. Regions where the AATSR 11 μm channel is likely to saturate are coloured black. May and June 1993.